

## OPEN

# Precision Mapping of Thalamic Deep Brain Stimulation Lead Positions Associated With the Microlesion Effect in Tourette Syndrome

Takashi Morishita, MD, PhD<sup>\*,†</sup>, Yuki Sakai, MD, PhD<sup>\*,†</sup>, Hitoshi Iida, MD, PhD<sup>‡</sup>, Saki Yoshimura, PhD<sup>\*,†</sup>, Shinsuke Fujioka, MD, PhD<sup>‡</sup>, Kazunori Oda, MD<sup>†</sup>, Saori C. Tanaka, PhD<sup>§</sup>, Hiroshi Abe, MD, PhD<sup>\*</sup>

<sup>\*</sup>Department of Neurosurgery, Fukuoka University Faculty of Medicine, Fukuoka, Japan; <sup>†</sup>ATR Brain Information Communication Research Laboratory Group, Kyoto, Japan; <sup>‡</sup>Department of Psychiatry, Fukuoka University Faculty of Medicine, Fukuoka, Japan; <sup>§</sup>Department of Neurology, Fukuoka University Faculty of Medicine, Fukuoka, Japan; <sup>¶</sup>Division of Information Science, Nara Institute of Science and Technology, Nara, Japan

This article was posted to medRxiv on September 12, 2022 under the title "Precision Mapping of Thalamic Deep Brain Stimulation Lead Positions Associated with the Microlesion Effect in Tourette Syndrome," <https://doi.org/10.1101/2022.09.07.22279661>.

\*Takashi Morishita and Yuki Sakai contributed equally to this work.

**Correspondence:** Takashi Morishita, MD, PhD, Department of Neurosurgery, Fukuoka University School of Medicine, Nanakuma 7-45-1, Jonan Ward, Fukuoka 814-0180, Japan. Email: [tmorishita@fukuoka-u.ac.jp](mailto:tmorishita@fukuoka-u.ac.jp)

**Received,** October 25, 2022; **Accepted,** February 10, 2023; **Published Online,** April 14, 2023.

Copyright © 2023 The Author(s). Published by Wolters Kluwer Health, Inc. on behalf of the Congress of Neurological Surgeons. This is an open access article distributed under the terms of the Creative Commons Attribution-Non Commercial-No Derivatives License 4.0 (CCBY-NC-ND), where it is permissible to download and share the work provided it is properly cited. The work cannot be changed in any way or used commercially without permission from the journal.

**BACKGROUND:** The microlesion effect refers to the improvement of clinical symptoms after deep brain stimulation (DBS) lead placement and is suggested to indicate optimal lead placement. Very few studies have reported its implications in neuropsychiatric disorders.

**OBJECTIVE:** To evaluate the magnitude of the microlesion effect in Tourette syndrome and the relationship between the microlesion effect and the anatomic location of implanted DBS leads.

**METHODS:** Six male patients were included. Their median age at surgery and follow-up period were 25 years (range, 18-47) and 12 months (range, 6-24), respectively. All patients were videotaped pre- and postoperatively, and tic frequencies were counted. We also analyzed the precision of lead placement and evaluated the normative connectome associated with the microlesion area.

**RESULTS:** The microlesion effect was observed as an improvement in tic symptoms in all patients, and the long-term clinical outcomes were favorable. The median motor tic frequency was 20.2 tics/min (range, 9.7-60) at baseline and decreased to 3.2 tics/min (1.2-11.3) in patients on postoperative day 1 ( $P = .043$ ) and to 5.7 tics/min (range, 1.9-16.6) in patients on postoperative day 7 ( $P = .028$ ). Phonic tic tended to improve immediately after surgery although the changes were not significant. Image analyses revealed that the precise position of the electrode was directed toward the anteromedial centromedian nucleus. Normative connectome analysis demonstrated connections between improvement-related areas and wide areas of the prefrontal cortex.

**CONCLUSION:** This study shows that the microlesion effect may seem as an immediate improvement after optimal DBS lead placement in patients with Tourette syndrome.

**KEY WORDS:** Tourette syndrome, Deep brain stimulation, Thalamus, Adverse events, Microlesion effect

Neurosurgery 00:1-9, 2023

<https://doi.org/10.1227/neu.0000000000002484>

**ABBREVIATIONS:** ANTs, Advanced Normalization Tools; CCA, complete case analysis; CM, centromedian; ET, essential tremor; F/U, follow-up; IPG, implantable pulse generator; MI, mean imputation; PD, Parkinson's disease; PW, pulse width; TS, Tourette syndrome; VTA, volume of tissue activated; YGTSS, Yale Global Tic Severity Scale.

Supplemental digital content is available for this article at [neurosurgery-online.com](https://neurosurgery-online.com).

Tourette syndrome (TS) is characterized by tic movements that rarely result in a debilitating state. Deep brain stimulation (DBS) may be indicated in patients with severe symptoms refractory to medical and behavioral therapies. Since the success of the first reported application of DBS to TS,<sup>1</sup> the clinical efficacy of the method has been confirmed in many reports.<sup>2-4</sup>

Although various targets including the centromedian (CM) thalamic nucleus are suggested to be equally effective,<sup>3,4</sup> the

therapeutic effects differ among patients. Although lead misplacement has potentially been linked to DBS failure,<sup>5</sup> very few reports mention the possibility of DBS failure for TS.<sup>6</sup> Because identification of the structure of the thalamic target is usually difficult in images, determination of the lead misplacement in thalamic DBS for TS is challenging, unless the misplacement is obvious. A recent multicenter analysis reported the preferred anatomic locations for TS-DBS<sup>7</sup> although the ideal position of the DBS electrode remains unclear.

The microlesion effect has been reported as a clinical sign of optimal lead placement in DBS for essential tremor (ET) and Parkinson's disease (PD).<sup>8,9</sup> Here, we hypothesized that a "sweet spot" area is associated with the microlesion effect of lead placement and optimal electrical stimulation in patients undergoing thalamic DBS for severe TS. Thus, this study evaluated the relationship between the microlesion effect and the anatomic location of implanted DBS leads in these patients.

## METHODS

### Study Design

The clinical data of the patients were prospectively recorded, and the data were linked to the neuroimaging data. The study protocol was approved by the institutional review board, and informed consent was obtained from all participants. Consecutive patients undergoing CM thalamic DBS in our department from January 2020 to December 2021 were included in this study. Because there has been no specific recommendation concerning the target selection for TS,<sup>10</sup> we selected CM thalamic DBS in this study as this has been the most commonly used approach.<sup>4,7</sup> In our facility, DBS therapy is indicated for patients  $\geq 12$  years of age with severe medication-refractory symptoms. A multidisciplinary evaluation was performed in all patients, as recommended by recent guidelines.<sup>6,11</sup>

The primary outcome measure was tic frequency evaluated in video recordings. We videotaped patients on postoperative days (PODs) 1 and 7 in the off-DBS condition to evaluate the microlesion effect and at a 6-month follow-up in the on- and off-DBS conditions. Study participants were hospitalized for a 6-month follow-up to monitor in case they could not tolerate the off-DBS condition. After videotape recording in the on-DBS condition and a 24-hour washout period, the patients were videotaped again in the off-DBS condition. During each session, the patients were left alone in a quiet room with a video camera and videotaped for at least 5 minutes. All patients were aware of the DBS conditions, but tic frequency was determined by a blinded rater (physical therapist). We also evaluated clinical outcomes with the Yale Global Tic Severity Scale (YGTSS)<sup>12</sup> both preoperatively and after surgery. In addition, adverse events were recorded. During the 6-month study period, the medications were unchanged, except in 1 patient (Case 6).

### Surgical Procedure

High-resolution MRI was conducted. Stereotactic planning for DBS lead placement was performed using iPlan Stereotaxy stereotactic planning software (Brainlab). The MRI sequences were fused automatically, and the mid-commissural point was defined to anchor the Cartesian coordinate system. The trajectory was determined according to the visualized thalamic structures and safe insertion angle.<sup>6,13,14</sup>

In this study, simultaneous bilateral DBS lead implantation (model 3387) was performed under C-arm guidance without microelectrode recording and only one macro-pass was performed on each hemisphere. We implanted an implantable pulse generator (IPG) on the same day (Activa RC for Cases 1 and 2; Percept PC from Case 3 on; Medtronic). All patients underwent the lead implantation while asleep under general anesthesia or deep sedation and the IPG implantation under general anesthesia.

Computed tomography (CT) was used to identify the lead location on POD 9. The CT image was fused with a preoperative scan to rule out lead misplacement. In cases where lead misplacement was diagnosed, additional surgery was performed during the same admission period.

### DBS Programming

Electrical stimulation was initiated 2 weeks after DBS surgery to activate the second-most ventral contacts bilaterally. Each patient was instructed to attend our DBS clinic once a month for a 6-month follow-up, and the stimulation intensity was gradually increased. If the stimulation parameter reached the maximum intensity within the therapeutic window in a single monopolar setting, the adjacent contact was activated to apply interleaving, multiple monopolar, or bipolar stimuli.

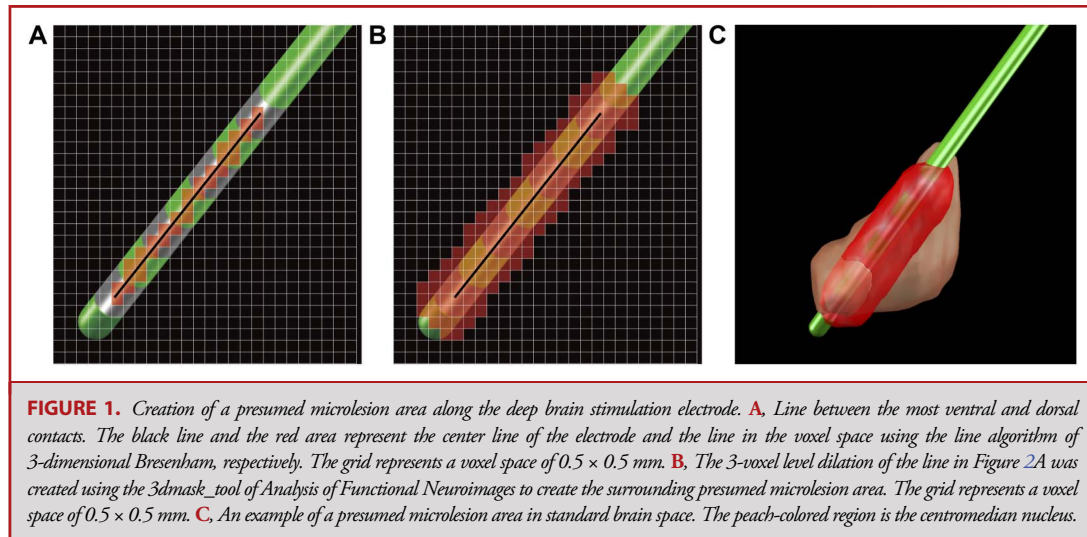
### Image Processing

We used Lead-DBS (<http://www.lead-dbs.org/>) to preprocess imaging data.<sup>6,15,16</sup> We coregistered images inclusive of postoperative CT and preoperative MR images linearly to the preoperative T1-weighted images using SPM software (<https://www.fil.ion.ucl.ac.uk/spm/software/spm12/>). To minimize the nonlinear bias associated with DBS surgery, the registration between preoperative T1WI and postoperative CT was refined using linear registration within the target region of interest in the sub-cortex.<sup>17</sup> We normalized all data to standard Montreal Neurological Institute space. The procedure was conducted using whole-brain nonlinear SyN registration in Advanced Normalization Tools (ANTs, <http://stnava.github.io/ANTs/>)<sup>18</sup> with the "effective (low variance)" setting and with subcortical refinement performed in Lead-DBS.<sup>16</sup> We automatically prereconstructed electrode trajectories and contacts using the Precise and Convenient Electrode Reconstruction for Deep Brain Stimulation algorithm<sup>19</sup> and manually adjusted them with Lead-DBS. Subject-independent 3-dimensional atlases of the thalamic nuclei were applied to evaluate the lead trajectory and contact positions.<sup>20</sup>

### Creation of the Presumed Microlesion Area

Precise identification of microlesion areas is difficult, so we assumed that microlesion areas would form around the electrode trajectories and create a presumed microlesion area. All the following procedures were performed in a voxel space of  $0.5 \times 0.5 \times 0.5$  mm.

First, we delineated the line between the most ventral and dorsal contacts identified using the Precise and Convenient Electrode Reconstruction for Deep Brain Stimulation algorithm. Because we needed to represent this line in voxel space, we used the line algorithm of 3D Bresenham (Figure 1A). We then performed a 3-voxel level dilation of this line using the 3dmask\_tool of Analysis of Functional Neuroimages<sup>21</sup> to create the surrounding presumed microlesion area, considering the microhemorrhage and edema based on a postmortem brain study reporting the range of neuronal loss surrounding the electrode (Figure 1B).<sup>22</sup> An example of a presumed microlesion area in standard brain space is shown in Figure 1C. Because the volume of data was limited, we used ANTs to nonlinearly transform the presumed microlesion areas in the



right hemisphere into those in the left hemisphere. All presumed microlesion areas were pooled across the hemispheres as left-sided areas.

To precisely evaluate the spatial overlap of the microlesion areas between patients, we assessed the percentage overlap of all microlesion areas. We also performed 2- and 4-voxel level dilations to confirm the similarity of overlapping areas (**Supplemental Digital Content**, <http://links.lww.com/NEU/D772>). To further evaluate the relationship between microlesion area and symptom improvement, we calculated the rate of symptom improvement on POD 7 relative to the preoperative severity. We calculated the improvement rate separately for motor and phonic tics and used the mean value. The median value among patients was assigned to each voxel in overlapping areas. When a presumed microlesion area of an electrode did not contain a voxel, its voxel improvement rate was regarded as 0. We defined the depicted region as an improvement-related area.

### Normative Connectome Analysis

To characterize the brain connectome from the microlesion area and reveal how microlesions affect the entire brain, we applied the population-averaged atlas of the macroscale human structural connectome derived from diffusion-weighted imaging data ( $N = 842$ , Human Connectome Project).<sup>23</sup> We evaluated the fiber tracts passing through the improvement-related area and assessed how many structural fibers are connected to each brain area determined by the Harvard-Oxford cortical/subcortical atlases<sup>24</sup> in conjunction with the Automated Anatomical Labeling atlas cerebellum.<sup>25</sup> All small Automated Anatomical Labeling-defined cerebellar parcels were integrated into a single binarized parcel.

### Statistical Analysis

We used the Wilcoxon signed-rank test to compare the pre- and post-DBS clinical scores of the YGTSS and tic frequencies. Statistical analyses

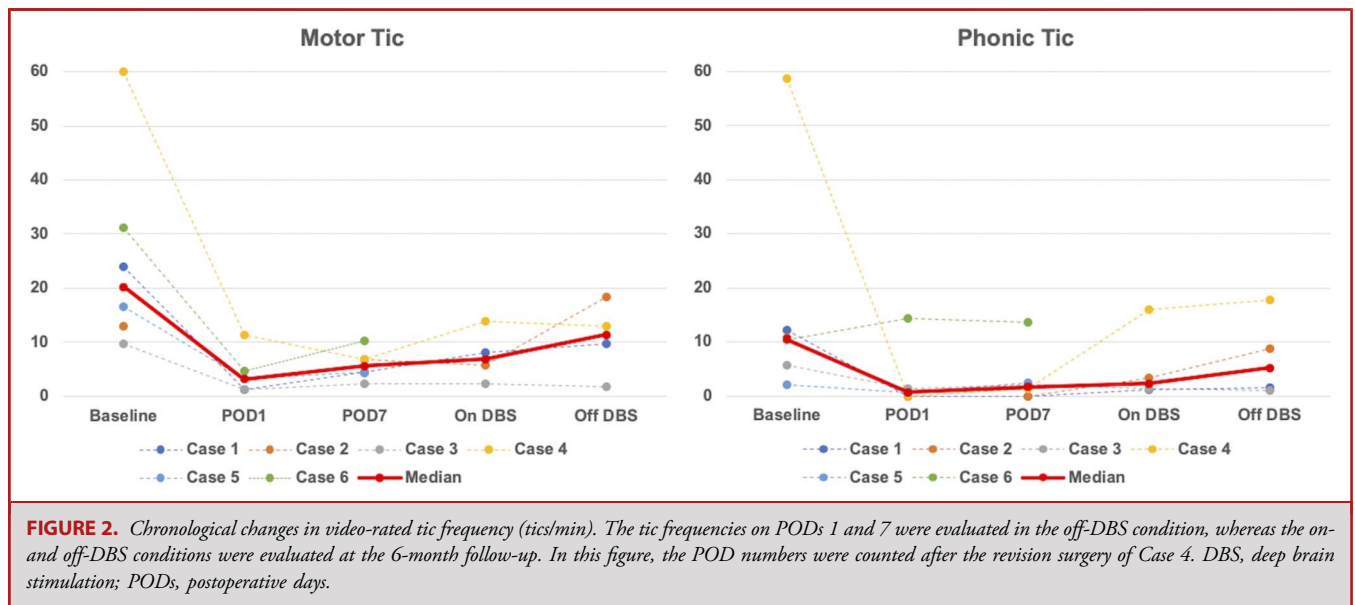


**TABLE 1. The Chronological Changes in the Tic Frequency on Video Rating**

Case	Motor tic frequency on video rating (tics/min)					Phonic tic frequency on video rating (tics/min)				
	Baseline	POD1	POD7	On DBS (6 mo)	Off DBS (6 mo)	Baseline	POD1	POD7	On DBS (6 mo)	Off DBS (6 mo)
1	23.9	1.2	4.5	8.1	9.7	12.1	0	0	1.2	1.5
2	12.9	NA	6.9	5.7	18.4	10.7	NA	0	3.3	8.8
3	9.7	1.2	2.4	2.4	1.8	5.7	1.3	2	1.3	1.0
4	>60	11.3	6.8	13.8	13	58.7	0	1.3	15.9	17.8
5	16.5	3.2	4.4	NA	NA	2	0.7	2.5	NA	NA
6	31.1	4.7	10.3	4.6	NA	10.3	14.4	13.7	1	NA
Median	20.2	3.2	5.7	6.9	11.4	10.5	0.7	1.65	2.3	5.2
P-value (CCA)	NA	.028	.028	.028	.046	NA	.075	.12	.028	.046
		.043		.043	.14		.14		.043	.068
P-value (MI)	NA	.028	NA	.028	.046	NA	.075	NA	.046	.17

CCA, complete case analysis; DBS, deep brain stimulation; MI, mean imputation; NA, not available; PODs, postoperative days.

were performed using SPSS version 21.0 (IBM Corp), and  $P < .05$  indicates statistical significance. To address the missing data, we performed a mean imputation (MI) in addition to complete case analysis (CCA).

## RESULTS

### Clinical Outcomes

This study included 6 male participants. The median age at the onset of TS and surgery was 8 years (range, 3-9) and 25 years (range, 18-47), respectively. The median follow-up period was 12 months

(range, 6-24). Video evaluation was performed during hospitalization immediately after DBS surgery in all 6 participants, but just 4 of the six participants (Cases 1-4) completed the planned 6-month follow-up in both on- and off-DBS conditions. One patient had been lost to follow-up for 6 months, and another could not complete the 6-month video rating in the off-DBS condition. However, there were no missing data for image analyses.

The microlesion effect was observed as an improvement in tic frequency in all patients. The median motor tic frequency was 20.2 tics/min (range, 9.7-60) at baseline and decreased to 3.2 tics/min (range, 1.2-11.3) on POD 1 (CCA:  $P = .043$ ; MI:  $P = .028$ ) and

**TABLE 2. Patient Demographics and YGTSS Scores**

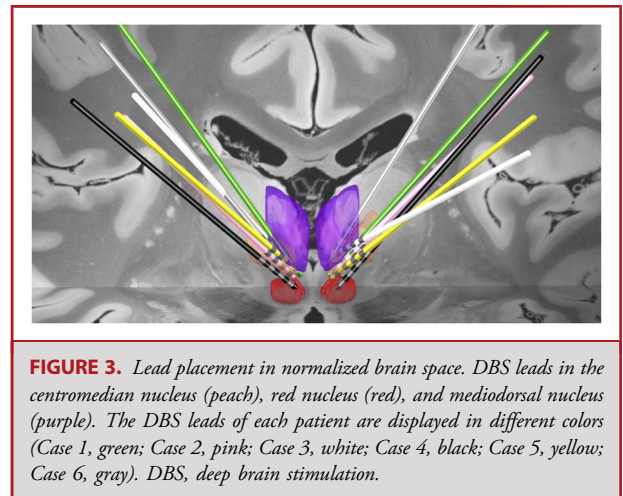
Case	Sex	Age at onset	Age at surgery	F/U period (mo)	YGTSS severity motor			YGTSS severity phonic			YGTSS impairment		
					Baseline	6 mo	Last F/U	Baseline	6 mo	Last F/U	Baseline	6 mo	Last F/U
1	Male	9	18	24	23	5	3	20	7	0	40	10	0
2	Male	9	26	24	44	9	7	21	12	7	50	30	20
3	Male	8	22	12	22	7	6	15	7	6	50	30	10
4	Male	3	34	12	22	0	8	19	8	8	40	10	20
5	Male	8	24	10 <sup>a</sup>	25	NA	12	14	NA	8	50	NA	40
6	Male	7	47	6	24	7	7	21	7	7	50	30	30
Median		8	25	12	23.5	7	7	19.5	7	7	50	30	20
P value (CCA)	NA	NA	NA	NA	NA	.043	.028	NA	0.043	.027	NA	.038	.027
P value (MI)	NA	NA	NA	NA	NA	.028	NA	NA	.028	.027	NA	.026	NA

CCA, complete case analysis; F/U, follow-up; MI, mean imputation; NA, not available; YGTSS, Yale Global Tic Severity Scale.

<sup>a</sup>Case 5 came back to regular follow-up 6 months after surgery, and the YGTSS scores were evaluated at the 10-month follow-up visit.

5.7 tics/min (range, 1.9-16.6) on POD 7 (CCA:  $P = .028$ ; MI: 0.028). However, no improvement in phonic tics was observed during the immediate postoperative period in either of the two patients (Cases 5 and 6). The median phonic tic frequency was 10.5 tics/min (range, 2.0-58.7) at baseline and decreased to 0.7 tics/min (range, 0-14.4) on POD 1 (CCA:  $P = .14$ ; MI:  $P = .075$ ) and 2.25 tics/min (range, 1.3-13.7) on POD 7 (CCA:  $P = .17$ ; MI:  $P = .12$ ). At the 6-month evaluation, the motor and phonic tic frequencies in the on-DBS condition were 6.9 tics/min (range, 2.4-13.8) and 2.3 tics/min (range, 1.0-15.9), respectively. These scores were significantly lower than those at baseline (motor:  $P = .043$  [CCA] and  $P = .028$  [MI]; phonic:  $P = .043$  [CCA] and  $P = .046$  [MI]). In addition, the motor and phonic tic frequencies in the off-DBS condition were 11.4 tics/min (range, 1.8-18.4) and 5.2 tics/min (range, 1.0-17.8), respectively. These scores were not significant but tended to be lower than those at baseline (motor:  $P = .14$  [CCA] and  $P = .046$  [MI]; phonic:  $P = .068$  [CCA] and  $P = .17$  [MI]). The chronological changes are shown in Figure 2 and Table 1. The stimulation parameters at the last follow-up are summarized in Table 1.

The median YGTSS motor and phonic scores improved from 23.5 (range, 22-44) and 19.5 (range, 14-21) at baseline to 7.0 (range, 3-12) ( $z = -2.20$ ,  $P = .028$ ) and 7.0 (range, 0-8) ( $z = -2.20$ ,  $P = .027$ ) at the last follow-up, respectively. The median YGTSS impairment score improved from 50 (range, 40-50) to 20 (range, 0-40) ( $z = -2.20$ ,  $P = .028$ ). The clinical outcomes are summarized in Table 2, and the stimulation parameters at the last follow-up are summarized in Table 3.



### Adverse Events

Surgical adverse events included wound dehiscence treated with surgical debridement (Case 3). Temporary stimulation-induced depression was also reported in the same patient. Lead misplacement on the left was diagnosed in Case 4 on POD 9 because the lead was more than 2 mm apart from the intended trajectory despite the appearance of microlesion effects; therefore, the patient underwent revision surgery on POD 12 before discharge. We excluded misplaced leads from the imaging

**TABLE 3.** The Stimulation Parameters at Last Follow-up

Case	Left					Right				
	Cathode	Anode	PW ( $\mu$ s)	Frequency (Hz)	Amplitude (mA)	Cathode	Anode	PW ( $\mu$ s)	Frequency (Hz)	Amplitude (mA)
1 <sup>a</sup>	2	Case	90	125	3.8	10	Case	90	125	3.5
	3	Case	60	125	2.8	11	Case	60	125	2.8
2	1	3	210	210	1.6	9	11	210	210	1.6
3 <sup>b</sup>	1	Case	150	180	1.9	10	Case	150	180	1.9
	2	Case	150	180	0.8	11	Case	150	180	0.8
4 <sup>b</sup>	1	Case	100	145	1.2	9	Case	100	145	1.2
	2	Case	100	145	1.3	10	Case	100	145	1.3
	3	Case	100	145	1.4	11	Case	100	145	1.4
5 <sup>b</sup>	2	Case	90	130	1.8	9	Case	90	130	1.8
	3	Case	90	130	0.3	10	Case	90	130	0.3
6 <sup>a</sup>	2	Case	90	125	1.8	10	Case	90	125	1.8
	3	Case	100	125	2.1	11	Case	100	125	2.1

PW, pulse width.

<sup>a</sup>Interleaving stimulation settings were applied.

<sup>b</sup>Multimonopolar settings were applied.



analysis. Another patient (Case 6) experienced intracerebral hemorrhage along the left DBS electrode because of severe self-injurious tics. To prevent expansion of the hemorrhage, we had to sedate the patient for several days and increase the medication and stimulation intensity to control the violent tics.

Stereotactic Precision and Connectome Images

The DBS lead locations in normalized brain space are shown in Figure 3. The precision analysis showed that the presumed microlesion areas for 8 of 12 DBS electrodes (75%) overlapped along

the electrode trajectory through the ventromedial area of the ventral lateral nucleus to the anteromedial area of the CM nucleus (Figure 4A). This result was commonly obtained from 2- to 4-voxel level dilatation analyses (Supplemental Digital Content, <http://links.lww.com/NEU/D772>). Further analysis showed that the precise electrode position associated with tic reduction evaluated on POD 7 was centered on the anteromedial CM nucleus (Figure 4B). Normative connectome analysis showed connections between the improvement-related area and wide areas of the prefrontal cortices and globus pallidus (Figure 5).

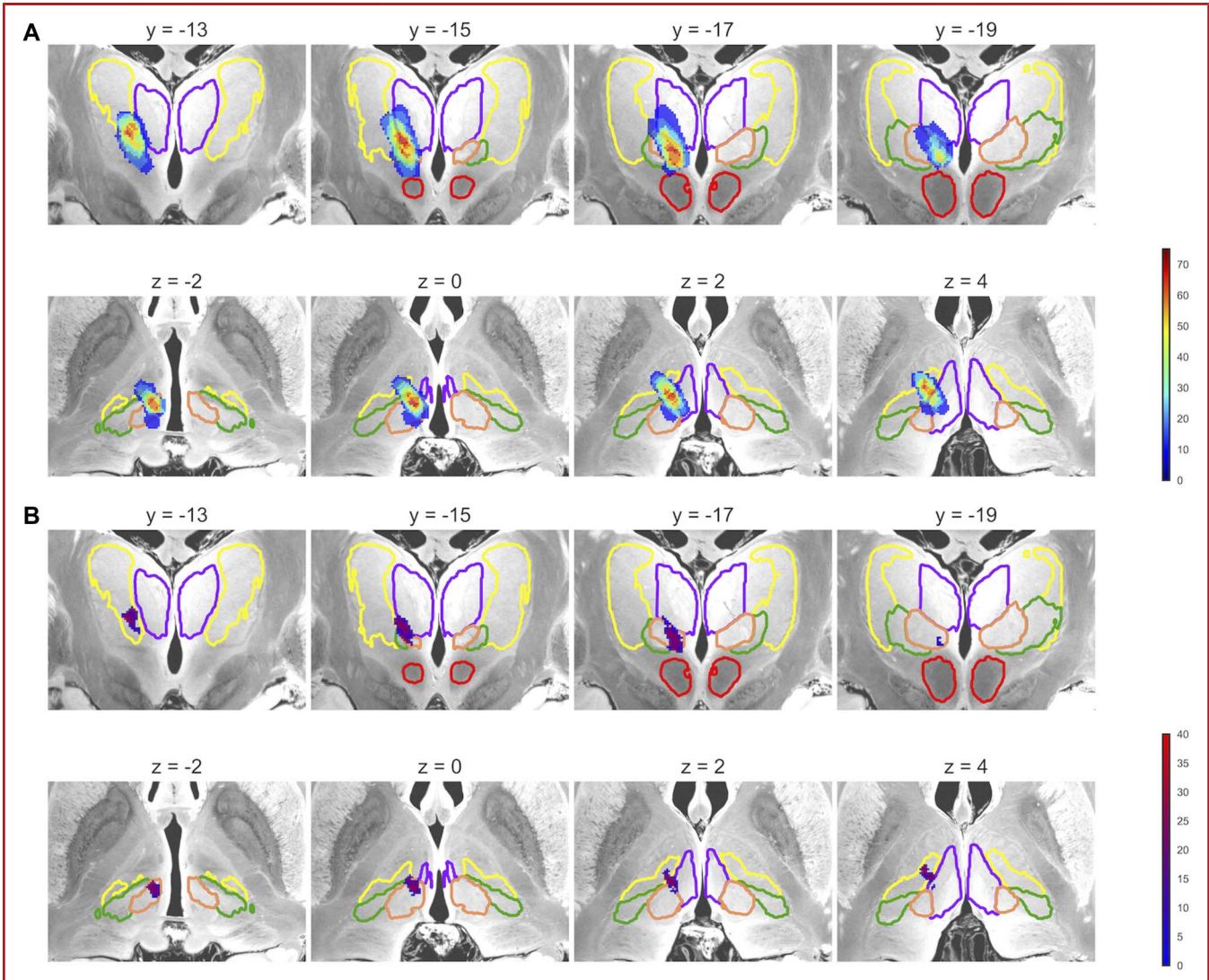


**FIGURE 4.** Precision mapping of implanted deep brain stimulation electrodes in an atlas. The upper and lower panels are the coronal and axial planes, respectively. Brain areas surrounded by a colored line represent the thalamic nuclei (centromedian nucleus, peach; red nucleus, red; mediodorsal nucleus, purple). The numbers above each panel are the Montreal Neurological Institute coordinates. **A.** Heat map of the microlesion area overlaps. The color bar represents the percentage of overlap among patients. **B.** Improvement-related area. The color bar represents the percentage improvement in tic symptoms.

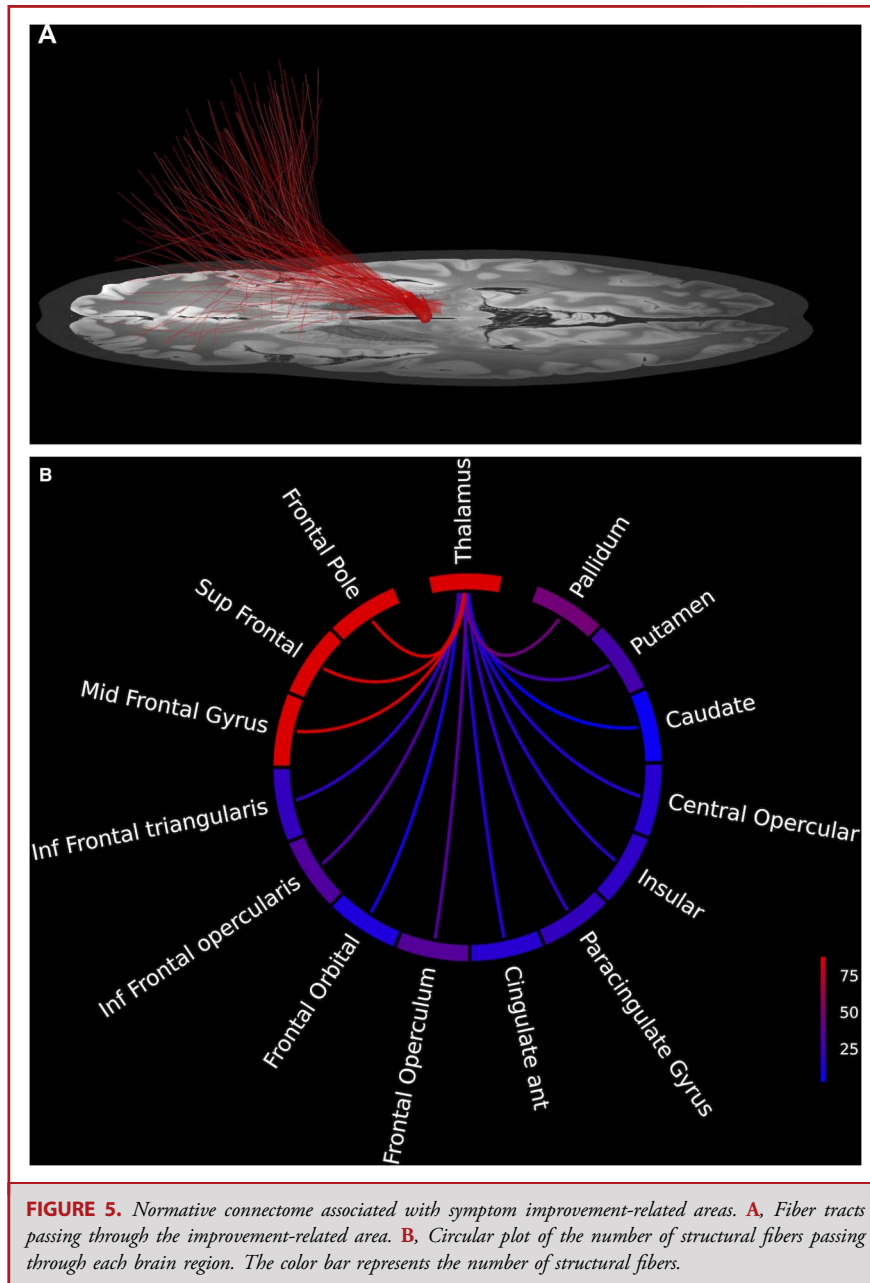


**FIGURE 5.** Normative connectome associated with symptom improvement-related areas. **A**, Fiber tracts passing through the improvement-related area. **B**, Circular plot of the number of structural fibers passing through each brain region. The color bar represents the number of structural fibers.

## DISCUSSION

This study investigated microlesion effects in patients with severe TS and the associated thalamic region. Our findings indicate that microlesion effects may potentially indicate the optimal lead placement. In cases where a strong microlesion effect is observed immediately after DBS surgery, DBS effects may seem to be lost over time if the stimulation parameters are not appropriate. Ideally, stimulation parameters should be programmed to focus on the sweet spot to avoid stimulation-induced adverse effects.

The microlesion effect is considered to result from edema, microhemorrhage, and the disruption of cells and/or fibers along the trajectory of DBS electrodes. The microlesion effect may even persist 6 months after surgery,<sup>8,9</sup> and in some cases, symptoms may be completely abolished without stimulation.<sup>26</sup> The chronological changes presented in Figure 2 were similar to those presented in the literature concerning the microlesion effects in ET and PD.<sup>8,9</sup> In addition, a randomized controlled trial of PD DBS demonstrated that the microlesion effect contributed to the decline of letter fluency at the 3-month visit after surgery.<sup>27</sup>

Similarly, the long-lasting microlesion effect may partly explain why the tic frequency in the off-DBS condition in our cases was lower than that in the baseline level even after 24 hours of stimulation washout although it is possible that neuroplasticity might have been induced by chronic electrical stimulation.

Previous studies reported that the sweet spot could be the anterior border of the CM nucleus and the medial area of the ventral lateral nucleus as the optimal stimulation area in other studies.<sup>2,6,28</sup> This study further supports this possibility. Furthermore, the normative connectome associated with the microlesion effect has components common to the connectome associated with the volume of tissue activated (VTA) of the therapeutic stimulation area; therefore, we consider that the presumed microlesion area in this study may include the sweet spot.

Normative connectome analysis has been increasingly used as a reliable research tool in DBS. As shown in this study and previous studies,<sup>6,15</sup> the normative connectome supports the interpretation of clinical effects and potentially guides DBS programming to induce therapeutic effects. Obtaining high-quality diffusion tensor images preoperatively is challenging especially in patients with TS with severe tic movements and requires clinical efforts to sedate such a patient. Furthermore, a recent study showed similar quality in analytical data between normative and patient-specific connectomes.<sup>29</sup> Therefore, we consider that the application of normative connectome analysis in this study is a reasonable option to support the findings of precision mapping.

It should also be noted that DBS surgery is usually performed bilaterally for neuropsychiatric diseases. However, there is a controversy regarding laterality.<sup>30,31</sup> Interestingly, one patient (Case 4) in our cohort showed clinical improvement immediately after the first surgery although the DBS electrode was misplaced on one side. In addition, the patient showed further improvement after revision surgery. In this context, there is a possibility that unilateral or staged surgery may be beneficial in selected patients, but no conclusion can be reached here. In addition, a case of lead misplacement was reported in a previous study,<sup>6</sup> and this issue could raise concern regarding the difficulty of precise lead placement in the CM thalamic DBS procedure. We consider that a lead misplacement may be suspected if DBS electrodes were implanted asymmetrically.

## Limitations

Although our study suggests the potential sweet spot of lead implantation in severe medication-refractory TS, it has several limitations. Only 6 patients were enrolled in this study, and 2 patients could not complete the full evaluations. Regarding the imaging study, we assumed and defined the microlesion area as a constant volume among patients; however, this may not be accurate because of the heterogeneity of the density of brain tissue or other biological factors. In addition, because we attempted to identify the sweet spot from the overlaps of the presumed microlesion areas, it is possible that we might have missed the true sweet spot. To address these limitations, multicenter studies with larger numbers of patients are needed to confirm our findings.<sup>4,7,32</sup>

## CONCLUSION

This study showed that the microlesion effect may seem as an immediate improvement after DBS lead placement in TS as reported in PD and ET. Our results support the existence of sweet spots for tic suppression in patients with severe TS. Clinicians should pay attention to programming sessions in the clinical setting. Further studies with greater patient numbers are required.

## Funding

This study was partially supported by the Japan Society for the Promotion of Science (JSPS) Grant-in-Aid for Scientific Research (C) (Grant number: 18K08956), the Central Research Institute of Fukuoka University (Grant number: 201045), Takeda Science Foundation, JSPS KAKENHI Grants (Grant numbers: JP16H06396 and JP21H05172), AMED (Grant number: JP18dm0307008), and Medical Corporation KONISHI DAIICHI HOSPITAL.

## Disclosures

The authors have no personal, financial, or institutional interest in any of the drugs, materials, or devices described in this article.

## REFERENCES

1. Vandewalle V, van der Linden C, Groenewegen HJ, Caemaert J. Stereotactic treatment of Gilles de la Tourette syndrome by high frequency stimulation of thalamus. *Lancet*. 1999;353(9154):724.
2. Dowd RS, Pourfar M, Mogilner AY. Deep brain stimulation for Tourette syndrome: a single-center series. *J Neurosurg*. 2018;128(2):596-604.
3. Baldermann JC, Schuller T, Huys D, et al. Deep brain stimulation for Tourette syndrome: a systematic review and meta-analysis. *Brain Stimul*. 2016;9(2):296-304.
4. Martínez-Ramírez D, Jiménez-Shahed J, Leckman JF, et al. Efficacy and safety of deep brain stimulation in Tourette syndrome: the International Tourette syndrome deep brain stimulation public database and registry. *JAMA Neurol*. 2018;75(3):353-359.
5. Morishita T, Foote KD, Burdick AP, et al. Identification and management of deep brain stimulation intra- and postoperative urgencies and emergencies. *Parkinsonism Relat Disord*. 2010;16(3):153-162.
6. Morishita T, Sakai Y, Iida H, et al. Neuroanatomical considerations for optimizing thalamic deep brain stimulation in Tourette syndrome. *J Neurosurg*. 2022;136(1):231-241.
7. Johnson KA, Fletcher PT, Servello D, et al. Image-based analysis and long-term clinical outcomes of deep brain stimulation for Tourette syndrome: a multisite study. *J Neurol Neurosurg Psychiatry*. 2019;90(10):1078-1090.
8. Mann JM, Foote KD, Garvan CW, et al. Brain penetration effects of micro-electrodes and DBS leads in STN or GPi. *J Neurol Neurosurg Psychiatry*. 2009;80(7):794-798.
9. Morishita T, Foote KD, Wu SS, et al. Brain penetration effects of microelectrodes and deep brain stimulation leads in ventral intermediate nucleus stimulation for essential tremor. *J Neurosurg*. 2010;112(3):491-496.
10. Szejko N, Worbe Y, Hartmann A, et al. European clinical guidelines for Tourette syndrome and other tic disorders-version 2.0. Part IV: deep brain stimulation. *Eur Child Adolesc Psychiatry*. 2022;31(3):443-461.
11. Pringsheim T, Okun MS, Müller-Vahl K, et al. Practice guideline recommendations summary: treatment of tics in people with Tourette syndrome and chronic tic disorders. *Neurology*. 2019;92(19):896-906.
12. Storch EA, Murphy TK, Geffken GR, et al. Reliability and validity of the Yale Global Tic Severity Scale. *Psychol Assess*. 2005;17(4):486-491.
13. Morishita T, Higuchi MA, Saita K, Tsuboi Y, Abe H, Inoue T. Changes in motor-related cortical activity following deep brain stimulation for Parkinson's disease detected by functional near infrared spectroscopy: a pilot study. *Front Hum Neurosci*. 2016;10:629.



14. Morishita T, Higuchi MA, Kobayashi H, Abe H, Higashi T, Inoue T. A retrospective evaluation of thalamic targeting for tremor deep brain stimulation using high-resolution anatomical imaging with supplementary fiber tractography. *J Neurol Sci.* 2019;398:148-156.
15. Morishita T, Sakai Y, Mishima T, et al. Case report: GPi DBS for non-parkinsonian midline tremor: a normative connectomic comparison to a failed thalamic DBS. *Front Hum Neurosci.* 2021;15:709552.
16. Horn A, Li N, Dembek TA, et al. Lead-DBS v2: towards a comprehensive pipeline for deep brain stimulation imaging. *Neuroimage.* 2019;184:293-316.
17. Schonecker T, Kupsch A, Kuhn AA, Schneider GH, Hoffmann KT. Automated optimization of subcortical cerebral MR imaging-atlas coregistration for improved postoperative electrode localization in deep brain stimulation. *AJNR Am J Neuroradiol.* 2009;30(10):1914-1921.
18. Avants BB, Epstein CL, Grossman M, Gee JC. Symmetric diffeomorphic image registration with cross-correlation: evaluating automated labeling of elderly and neurodegenerative brain. *Med Image Anal.* 2008;12(1):26-41.
19. Husch A, V Petersen M, Gemmar P, Goncalves J, Hertel F. PaCER - a fully automated method for electrode trajectory and contact reconstruction in deep brain stimulation. *NeuroImage Clin.* 2018;17:80-89.
20. Ilinsky I, Horn A, Paul-Gilloteaux P, Gressens P, Verney C, Kultas-Ilinsky K. Human motor thalamus reconstructed in 3D from continuous sagittal sections with identified subcortical afferent territories. *eNeuro.* 2018;5(3):ENEURO.0060-18.2018.
21. Cox RW. AFNI: software for analysis and visualization of functional magnetic resonance neuroimages. *Comput Biomed Res.* 1996;29(3):162-173.
22. Henderson J, Rodriguez M, O'Sullivan D, et al. Partial lesion of thalamic ventral intermediate nucleus after chronic high-frequency stimulation. *Mov Disord.* 2004;19(6):709-711.
23. Yeh FC, Panesar S, Fernandes D, et al. Population-averaged atlas of the macroscale human structural connectome and its network topology. *Neuroimage.* 2018;178:57-68.
24. Makris N, Goldstein JM, Kennedy D, et al. Decreased volume of left and total anterior insular lobule in schizophrenia. *Schizophrenia Res.* 2006;83(2-3):155-171.
25. Tzourio-Mazoyer N, Landeau B, Papathanassiou D, et al. Automated anatomical labeling of activations in SPM using a macroscopic anatomical parcellation of the MNI MRI single-subject brain. *Neuroimage.* 2002;15(1):273-289.
26. Kondziolka D, Lee JY. Long-lasting microthalamotomy effect after temporary placement of a thalamic stimulating electrode. *Stereotact Funct Neurosurg.* 2004;82(2-3):127-130.
27. Okun MS, Gallo BV, Mandybur G, et al. Subthalamic deep brain stimulation with a constant-current device in Parkinson's disease: an open-label randomised controlled trial. *Lancet Neurol.* 2012;11(2):140-149.
28. Kakusa B, Saluja S, Barbosa DAN, et al. Evidence for the role of the dorsal ventral lateral posterior thalamic nucleus connectivity in deep brain stimulation for Gilles de la Tourette syndrome. *J Psychiatr Res.* 2021;132:60-64.
29. Wang Q, Akram H, Muthuraman M, et al. Normative vs. patient-specific brain connectivity in deep brain stimulation. *Neuroimage.* 2021;224:117307.
30. Huff W, Lenartz D, Schormann M, et al. Unilateral deep brain stimulation of the nucleus accumbens in patients with treatment-resistant obsessive-compulsive disorder: outcomes after one year. *Clin Neurol Neurosurg.* 2010;112(2):137-143.
31. Morishita T, Fayad SM, Goodman WK, et al. Surgical neuroanatomy and programming in deep brain stimulation for obsessive compulsive disorder. *Neuro-modulation.* 2014;17(4):312-319; discussion 319.
32. Schrock LE, Mink JW, Woods DW, et al. Tourette syndrome deep brain stimulation: a review and updated recommendations. *Mov Disord.* 2015;30(4):448-471.

## Acknowledgments

We would like to thank Dr Hisatomi Arima for supervising statistical analyses. T.M. and Y.S. contributed to the conceptualization, data collection and analysis, and manuscript writing. H.I., S.Y., and S.F. contributed to the data gathering and review of the manuscript. K.O. contributed to the statistical analysis. S.C.T. and H.A. supervised the study and reviewed the manuscript.

---

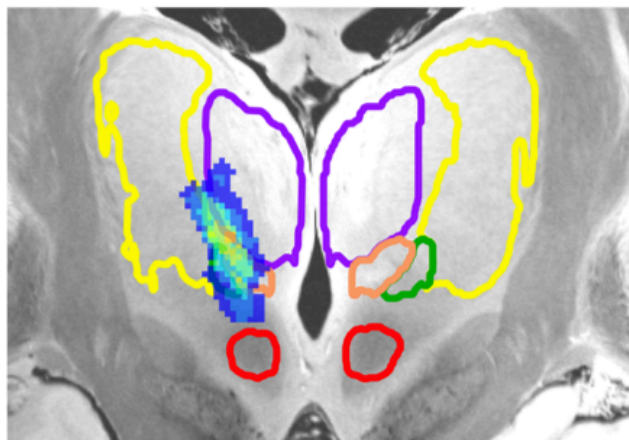
**Supplemental digital content** is available for this article at [neurosurgery-online.com](https://www.neurosurgery-online.com).

---

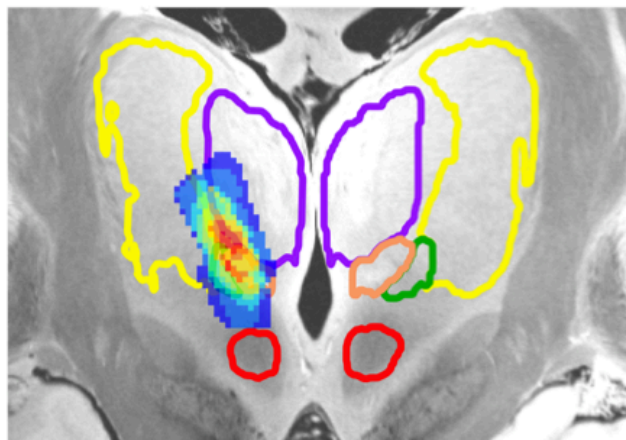
Comparison of different-level dilatation analyses of overlapping areas.

---

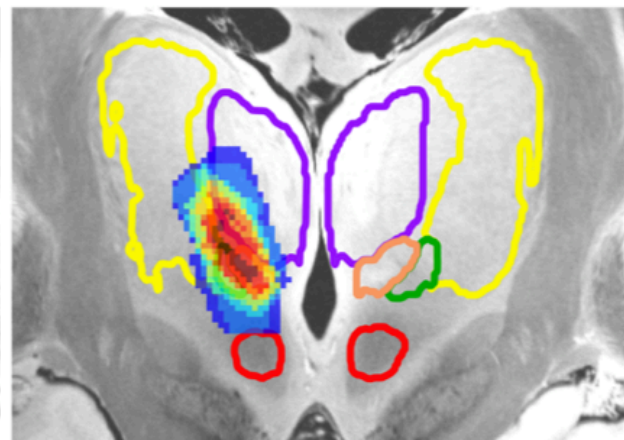
$y = -15$   
2-voxel level dilation



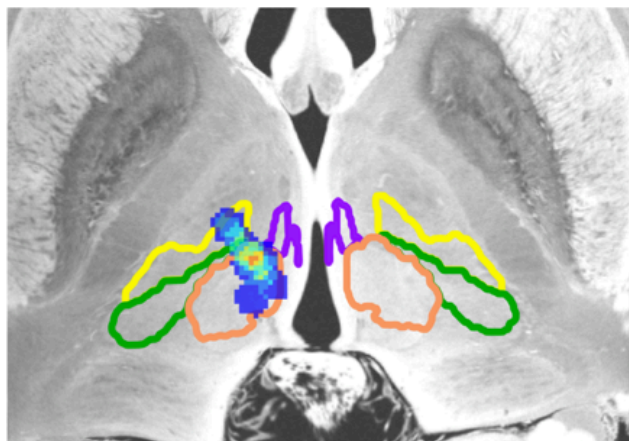
$y = -15$   
3-voxel level dilation



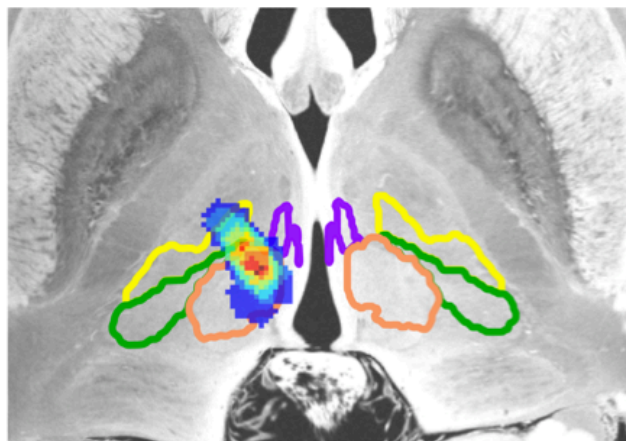
$y = -15$   
4-voxel level dilation



$z = 0$   
2-voxel level dilation



$z = 0$   
3-voxel level dilation



$z = 0$   
4-voxel level dilation

